Unimodal maps and order parameter fluctuations in the critical region

Y. F. Contoyiannis* and F. K. Diakonos†
Department of Physics, University of Athens, 15771 Athens, Greece
(Received 10 January 2007; revised manuscript received 3 August 2007; published 27 September 2007)

Recently it has been argued that the fluctuations of the order parameter of a system undergoing a second order transition, when considered as a time series, possess characteristic nonstochastic patterns at the critical point. These patterns can be described by a unimodal intermittent map (critical map) and are clearly distinguished from colored noise. In the present work we extend the method introduced in [Y. F. Contoyiannis, F. K. Diakonos, and A. Malakis, Phys. Rev. Lett. **89**, 035701 (2002)], in order to reveal universal properties in the deformation of the dynamics of the order parameter fluctuations when departing from the critical point. We show that the obtained systematic change in the order parameter fluctuation pattern can be observed in the critical region of thermal critical systems such as the mean field and the 3D Ising model. In addition, we consider the case of order parameter fluctuations near a tricritical point and we derive an associated characteristic deterministic behavior. A corresponding analysis in the $Z(3)$ model confirms our results. Thus, the method of critical fluctuations introduced previously and generalized here, provides us with a classification scheme allowing for the characterization of temporal fluctuations in an observed time series in terms of critical phenomena.

DOI: 10.1103/PhysRevE.76.031138 PACS number(s): 05.20.−y, 05.40.−a, 05.70.Jk

I. INTRODUCTION

In most theoretical studies the temporal fluctuations of the order parameter are simulated through a random walk in the space of microstates of the corresponding system. The basic characteristics of these stochastic processes are primarily determined through the requirement of approaching thermal equilibrium. Usually the appropriate random walks are generated applying efficient algorithms such as the Metropolis [1], the heat-bath or other more sophisticated approaches (for a review see [2,3]). The obtained fluctuations are, in general, of stochastic origin and there is no obvious connection between the simulated and the actual fluctuation time series in a real physical system. On the other hand, exactly at the critical point the relaxation time diverges and no characteristic time scale describing the variation of the order parameter exists. This implies the appearance of temporal self-similarity in the corresponding time series. As shown in [4,5], this self-similar behavior can be generated by a simple dynamical law, named critical map (CM), belonging to the class of intermittent maps. The dynamics of CM introduces in turn a critical exponent p_l capturing the self-similarity of the order parameter time series. In [5] an algorithm is developed for the calculation of this critical exponent. The appealing property of p_l is that it can be determined in a straightforward manner using a single time series of an observable characterizing the critical system. In addition, it can be easily defined also in the case of phase transitions out of equilibrium. The purpose of the present work is to extend the analysis presented in [4,5] in order to describe the dynamics of the order parameter fluctuations in the entire critical region, i.e., in the immediate neighborhood of the critical point where the relaxation time is large but finite. To achieve this, one has to construct a simplified version of CM combining the relevant dynamical properties with the correct reproduction of statistical features of the order parameter at the critical point. Then, as we will show below, by a simple modification of the constructed map the description of the order parameter fluctuations beyond the critical point is possible in a transparent way. The paper is organized as follows: in Sec. II we construct the aforementioned simplification of the CM giving emphasis on its self-consistency. To illustrate the latter we consider the case of a thermal critical system using as specific examples the mean field and the 3D Ising model. In Sec. III we generalize the map obtained in Sec. II in order to describe the dynamics of the order parameter as the control parameter is decreased from its critical value (broken phase). In Sec. IV we show how our approach can be further modified to enable a consistent modeling of the dynamics of the order parameter fluctuations in the case of a transition with a tricritical point. The consistency of the proposed dynamical map is checked using simulations of the $Z(3)$ model, which possesses such a critical behavior. Finally, in Sec. V we present our concluding remarks and give a possible outlook of our work.

II. SIMPLIFIED DESCRIPTION OF THE CRITICAL FLUCTUATION DYNAMICS

Recently it has been shown [4,5] that near the critical point the order parameter fluctuations, independently of the algorithm used in the simulation [12], develop a deterministic profile, which can be described by intermittent dynamics. Using a general parametrization of the critical effective action it is possible to derive a one-dimensional map—introduced in [4] as *critical map*—capable of reproducing several properties of the order parameter time series, such as, for example, the suitable defined laminar length distribution of the critical system. The proposed dynamics have been successfully revealed at the critical point of the 3D ferromag-

*ycont@vodafone.net.gr
†fdiakono@phys.uoa.gr

netic Ising system using two different algorithms (Metropolis and heat-bath) in the corresponding simulations [5]. Assuming certain smoothness constraints [4] the critical map can be simplified to

$$\phi_{n+1} = \phi_n + u\phi_n^z, \tag{1}$$

where ϕ is the order parameter (in 3D Ising model the space averaged magnetization), u is a parameter associated with the coupling constant of the effective action, and the exponent z is related to the critical isothermal exponent δ through $z=\delta+1$. Time (n) is measured in units of a resolution scale τ for which we only require that it is much smaller than the autocorrelation time of ϕ. The physical picture underlying Eq. (1) is that just after the symmetry breaking leading to the nonvanishing value of the order parameter, the vacuum state ($\phi=0$) of the system in the symmetric phase turns from a stable fixed point of the effective interaction into a marginally unstable one through a pitchfork bifurcation inducing the aforementioned intermittent dynamics. There is a universal property valid for any trajectory of the dynamical system (1): in the laminar region $0 \leq \phi \leq \phi_{\max}$, with $\phi_{\max} \approx (\frac{1}{zu})^{1/z-1}$ the dynamics are almost regular and the time intervals spent in this region are distributed according to the power law as follows:

$$P(l) \sim l^{-p_l}, \tag{2}$$

with $p_l = \frac{z}{z-1}$. Although ergodicity is a key property in the derivation of the exact critical map, the simplified dynamics (1) is not ergodic. Therefore it fails to describe some statistical properties of the order parameter (which the exact critical map does), such as, for example, its distribution for a given temperature, at the level of a single trajectory [13]. On the other hand, the simplified map (1) is much more handy than the exact, incorporating at the same time the essential part of the dynamics. To establish ergodicity of the simplified map one can add a noise term ϵ_n in the right-hand side of Eq. (1). However, the trivial addition of noise does not lead to dynamics capable of reproducing correctly the invariant density of the order parameter at the critical temperature. In particular, the characteristic plateau for order parameter values just above the marginally unstable fixed point $\phi^*=0$ requires the use of uniformly distributed ϵ_n. Even more, in order to avoid negative values of the order parameter, one should modify the map (1) as follows in order to achieve a consistent (and ergodic) dynamical description of the critical fluctuations of the order parameter:

$$\phi_{n+1} = |\phi_n + u\phi_n^z + \epsilon_n| \mathrm{mod}\ 1/2, \tag{3}$$

where ϵ_n is uniformly distributed in the interval $[-\epsilon_0, \epsilon_0]$. The noise amplitude ϵ_0 as well as the parameter u have to be fine tuned for the optimum reproduction of the order parameter distribution at the critical point. In particular, the value of ϵ_0 has to be chosen sufficiently small in order to avoid the deformation of the dynamics by noise but not too small in order to avoid the violation of ergodicity. In addition, using the optimized noise amplitude in the dynamics (3) one can ensure that the statistics of the laminar intervals (2) remains unaltered. Furthermore, choosing ϵ_0 and u appropriately it is

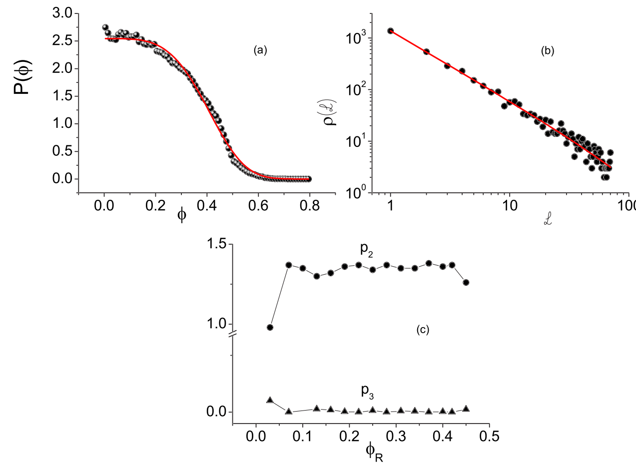

FIG. 1. (Color online) (a) The invariant density $P(\phi)$ produced through a single trajectory of the map (3) using $z=4$, $u=0.011$, $\epsilon_0=0.0175$, and $\phi_0=0$ (full circles). The fitting function $\tilde{P}(\phi)=c_1 e^{-c_2\phi^{c_3}}$ describes $P(\phi)$ for $c_3=4\pm0.11$ very well. This is in remarkable agreement with the theoretical expectation based on the free energy of a mean field universality class critical system [5]. (b) The distribution $\rho(\mathcal{L})$ of the laminar intervals in a typical trajectory of the map (3) shown using a log-log plot. The same trajectory as in (a) is used. The solid line is the linear fit leading to the calculation of the exponent p_2 ($p_2 \approx 1.35\pm0.01$). (c) The functions $p_2(\phi_R)$ and $p_3(\phi_R)$ calculated using a single trajectory of (3). An increase of p_3 leads to a decrease of p_2 and vice versa.

possible to reproduce the superexponential tail of the order parameter distribution characteristic for a critical system [5]. To illustrate this property we plot in Fig. 1(a) the invariant density produced through a single trajectory (500 000 iterations) of the map (3) using $z=4$ ($\delta=3$ for the isothermal critical exponent) corresponding to the description of the order parameter fluctuations of a system belonging to the widespread mean field universality class. In this case using the values $u=0.011$ and $\epsilon_0=0.0175$ one can reproduce very well the magnetization probability density of the critical system (solid line). The trajectory generated by (3) has as starting value $\phi_0=0$. It must be noted that the observed minor deviation cannot be corrected through increasing the length of the trajectory used in the calculation. This is due to the fact that the map (3) is only an approximation (valid for small ϕ values) of the exact critical map [4].

The calculation of the distribution $\rho(\mathcal{L})$ of the laminar intervals $\mathcal{L}$ is more complicated. The corresponding algorithm has been introduced in the previous works [5,6]. However, in order to be self-contained we repeat it briefly here. The laminar lengths $\mathcal{L}$ are defined as the time intervals spent in the laminar region, i.e., the linear neighborhood of a marginally unstable fixed point. The exact size of the laminar region is not known. Therefore it is treated as a free parameter in the calculation. A rough estimation of the laminar region can be obtained from the size of the plateau in the distribution $P(\phi)$. In fact we use as one end of the laminar domain the position of the fixed point (start of the plateau) (here $\phi_L=0$) and as the other end some value of ϕ at the edge of the plateau (ϕ_R). Fixing the limits ϕ_L, ϕ_R of the laminar region we determine the distribution $\rho(\mathcal{L})$ by calculating the sequence of sizes of the laminar intervals $\mathcal{L}$ counting the number of successive ϕ values fulfilling the condition $\phi_R \geq \phi_i \geq \phi_L$. We use the fitting function

$$\tilde{\rho}(\mathcal{L}) = p_1 \mathcal{L}^{-p_2} e^{-p_3 \mathcal{L}} \quad (4)$$

for an analytical approximation of $\rho(\mathcal{L})$ estimating the appropriate values of the fitting parameters p_1, p_2, and p_3 through a χ^2-minimization procedure. In general the exponents p_2 and p_3 depend on the choice of ϕ_R and have a competitive role. When p_3 is decreasing p_2 increases and vice versa. The function $p_3(\phi_R)$ possesses a minimum value at $\phi_R=\phi_R^*$ approaching $p_3 \approx 0$ while p_2 becomes maximum. Therefore for $\phi_R=\phi_R^*$ the distribution of the laminar lengths comes closer to a power law and the corresponding value of p_2 can be identified with the exponent p_l in Eq. (2). In some cases the maximum of p_2 is very broad allowing for statistical fluctuations which can be washed out by a suitable averaging. It should be noted here that for a thermal critical system the condition $p_l > 1$ (or equivalently, $p_2 > 1$) has to be fulfilled due to the fact that the exponent δ is positive definite. To illustrate the above analysis in a concrete example we show in Fig. 1(b) the distribution of laminar lengths obtained through a typical trajectory of the map (3) using the same parameters as in Fig. 1(a). The calculation is performed using $\phi_R=0.31$. The quality of the fit measured in terms of the coefficient of determination R^2 is excellent ($R^2=0.999$). The corresponding fit parameters take the values $p_2 = 1.35 \pm 0.012$, $p_3 = 0.005 \pm 0.003$ compatible with a power-law behavior of $\rho(\mathcal{L})$. In Fig. 1(c) we show the functions $p_2(\phi_R)$ and $p_3(\phi_R)$ determined using the same trajectory. In fact, as discussed above, there is a broad plateau of p_2 values. Averaging over the almost constant values (in order to suppress statistical fluctuations) leads to the mean value $\langle p_2 \rangle \approx 1.36$, which in turn gives $z \approx 4$. This result classifies the considered dynamics in the universality of the mean field theory ($p_l = 1.33$).

III. DYNAMICS OF FLUCTUATIONS BEYOND THE CRITICAL POINT

Let us now proceed to the main goal of the present work, which is the description of the order parameter fluctuation dynamics in an extented region around the critical point. It is straightforward to generalize the map (3) in order to construct effective dynamics incorporating the departure from the critical point. To achieve this step we introduce the parameter r in the linear term in Eq. (3) determining the stability properties of the fixed point at $\phi^*=0$. The resulting dynamical law takes the form

$$\phi_{n+1} = |r\phi_n + u\phi_n^z + \epsilon_n| \text{mod } 1/2. \quad (5)$$

Exactly at the critical point $r=1$, while as we depart from it, r increases. This change in the stability properties of the fixed point associated with the critical point deforms also, due to the corresponding symmetry breaking, the distribution of the order parameter. In the mean field universality class the Ginzburg-Landau free energy reads

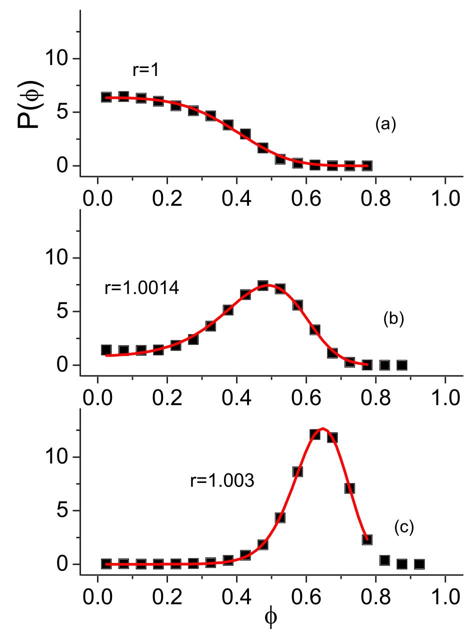

FIG. 2. (Color online) The distribution $P(\phi)$ for (a) $r=1$, (b) $r=1.0014$, and (c) $r=1.003$ obtained using a single trajectory of Eq. (5). The solid line is the fit result using the function $f(x)$ described in the text.

$$\Gamma[\phi] = \frac{1}{2} u_2 \phi^2 + u_4 \phi^4, \quad (6)$$

where $u_2 = a_0 t$ $\left(t = \frac{T-T_c}{T_c}\right)$ with $a_0 > 0$ and $u_4 > 0$. According to Eq. (6) the probability density of the order parameter ϕ is given by: $\rho(\phi) = \frac{e^{-\Gamma[\phi]}}{\int d\phi e^{-\Gamma[\phi]}}$. In fact this is exactly the form of the probability density, which we obtain by evoluting the map (5). This is shown in Figs. 2(a)–2(c), where we present for three different r values ($r=1$, $r=1.0014$, and $r=1.003$, respectively) the distribution of ϕ obtained using in each case a single trajectory with 500 000 iterations of Eq. (5) and initial condition $\phi_0=0$ (as before $u=0.011$ and $\epsilon_0=0.0175$).

The result for $r=1$ clearly resembles with very good accuracy the order parameter probability density at the critical point of the mean field universality class. The case $r=1.0014$ corresponds to the order parameter distribution for the phase of broken symmetry just below the mean field critical point. Finally, when $r=1.003$ the corresponding ϕ distribution describes the *cold* phase with large spontaneous magnetization. Inspired by Eq. (6) one can use the fitting function $f(x) = c \exp(ax^2 - bx^4)$ to describe the distributions in Figs. 2(a)–2(c). This can be performed for a large number of r values in order to obtain the dependence $a(r)$, $b(r)$. The results of this analysis are shown in Figs. 3(a) and 3(b).

It is interesting to note that the parameter a depends linearly on r while the parameter b displays a saturating behavior as r increases. Note that in the r dependence of the function $a(r)$ one recognizes two regions with slightly different slopes. The r value at the crossover corresponds to the T value for which the initial plateau region in the density $P(\phi)$ disappears. These findings are in full analogy to the depen-

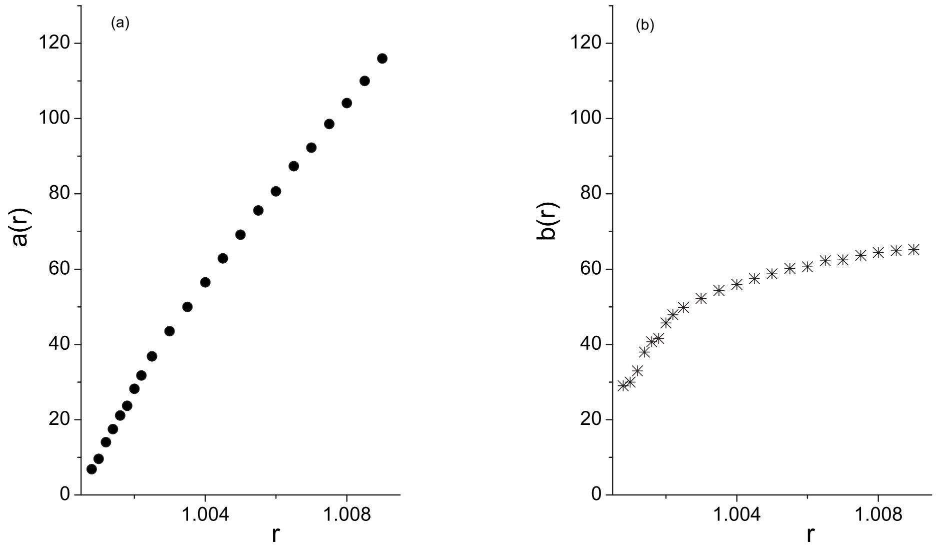

FIG. 3. The functions (a) $a(r)$ and (b) $b(r)$ obtained through the procedure described in Sec. II.

dence of the parameters u_2, u_4 of the free energy (6) on reduced temperature t [7]. This suggests that r is proportional to t since $a=\lambda_1 r+\lambda_2$ while $u_2=\frac{a_0}{2}t$ leading to $r=1-\frac{a_0}{2\lambda_1}t$. Note that, due to the minus sign, when T decreases r increases.

It must be noted that the qualitative behavior of the order parameter distribution for temperatures just below the critical one is the same in any thermal system undergoing a second order transition. This is clearly seen in the example of the 3D ferromagnetic Ising model as the temperature shrinks below the critical one. In Figs. 4(a)–4(c) we show the distribution of the mean magnetization for three different values of the temperature: (a) $T\approx T_c=4.545$, (b) $T=4.5$, and (c) $T=4.44$. The histograms are obtained through Monte Carlo simulation using the Metropolis algorithm [1] for a lattice of size $20\times 20\times 20$. A single random walk consisting of 220 000 steps is used. Spontaneous magnetization is established as the temperature decreases to values less than T_c. Although the system belongs to a different universality class (different value of the isothermal critical exponent $\delta\approx 5$) the similarity to the mean field case is obvious.

In fact this similarity is more exciting at the level of the order parameter fluctuations. In Fig. 5 we compare the distribution of the laminar intervals $P(\mathcal{L})$ for the 3D Ising model at $T=4.45$ with the corresponding distribution found for the map (5) at $r=1.002$.

The breakdown of the power-law behavior due to the gradual destruction of the self-similarity associated with the critical point is the main property characterizing the fluctuations of the order parameter in the subcritical region. To obtain an analytical estimation of $P(\mathcal{L})$ one can use the simplified form $\phi_{n+1}=r\phi_n+u\phi_n^z$ of the map (5). The related analysis is extensively given in the Appendix. The resulting distribution is

$$P(\mathcal{L}) = N\frac{e^{\mathcal{L}(z-1)(r-1)}}{[e^{\mathcal{L}(z-1)(r-1)}]^{z/(z-1)}-1}, \quad (7)$$

where N is a normalization constant. The function (7) behaves as a power law $P(\mathcal{L})\sim\mathcal{L}^{-z/(z-1)}$ for small values of $\mathcal{L}$ $(\mathcal{L}\ll\frac{1}{r-1})$ and decays exponentially $P(\mathcal{L})\sim e^{-\mathcal{L}(r-1)}$ for $\mathcal{L}\gg\frac{1}{r-1}$ in accordance with the behavior shown in Fig. 5. Thus the fluctuation pattern of the order parameter in the region just below the critical temperature characterized by the distribution (7) turns out to be a universal property of systems undergoing a second order transition.

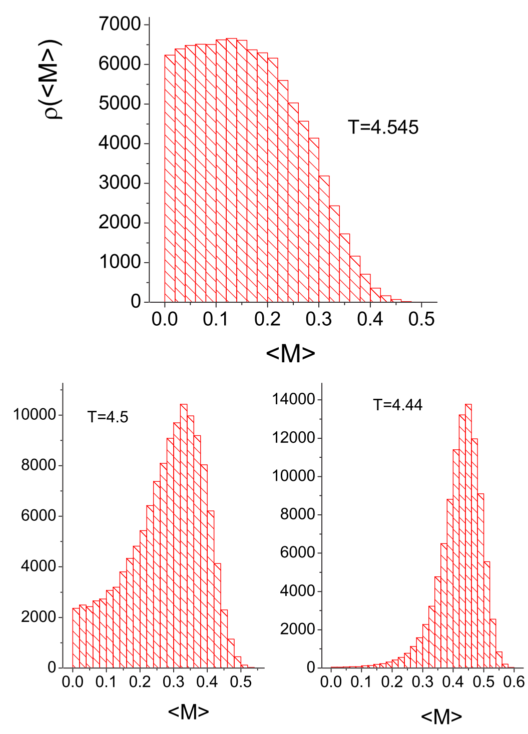

FIG. 4. (Color online) The distribution of the mean magnetization in the 3D ferromagnetic Ising model for (a) $T=4.54$, (b) $T=4.5$, and (c) $T=4.44$. The simulations are performed using the Metropolis algorithm on a 20^3 lattice.

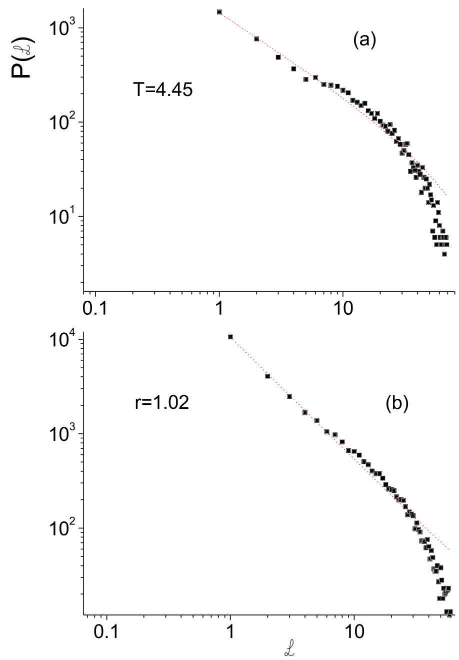

FIG. 5. (Color online) The distribution of the laminar intervals in the 3D Ising model for $T=4.44$ (a) compared with the corresponding quantity calculated using the map (5) with $r=1.002$ (b). The breakdown of the power-law behavior is clearly seen.

IV. FLUCTUATION DYNAMICS OF THE TRICRITICAL BEHAVIOR

As argued in [5,6,8] the calculation of the exponent p_2 using an experimentally observable time series is straightforward and can be used for a search of signatures of critical fluctuations in a wide class of complex systems. Such an analysis has been extensively performed in biological [6] and geophysical [9,8] systems. In these studies a frequently occurring scenario is when the distribution $P(\mathcal{L})$ obeys the law (4) with $p_2<1$ and p_3 of the order of 0.1. This case describes an intermediate phase between the critical power-law behavior and the exponential form characterizing short range correlated (in time) processes. In the language of critical phenomena this phase corresponds to a metastable state associated with the appearance of tricritical behavior. For such a system the effective action is no more scale-free depending on the order parameter in a polynomial form. As we will show below, an analogous generalization of the map (5) captures several characteristics of the tricritical state including the temporal fluctuations of the order parameter as described by the distribution $P(\mathcal{L})$. For a mean field theory ($z=4$) the proposed effective dynamics has the form

$$\phi_{n+1} = |r\phi_n + u_1\phi_n^2 + u_2\phi_n^4 + \epsilon_n| \text{mod } 1/2, \tag{8}$$

where ϵ_n is the noise term while the scale invariance of the mean field universality class is broken through the quadratic term in ϕ_n. It is straightforward to calculate the distribution of the sizes of the laminar intervals for the map (8). For a very narrow zone of r values just above $r=1$ and restricting the laminar region to the immediate neighborhood of the fixed point, the power-law characteristics in the distribution of laminar intervals remain valid. As r is increased beyond a critical value r_c no such laminar region can be found and the corresponding profile of $P(\mathcal{L})$ although keeping the power-law form does not possess critical characteristics any more since we obtain $p_2<1$. The power-law description of the laminar interval distribution for $r=1.09r_c$ is shown in Fig. 6(a). In fact the exact value of r_c depends on the other parameters in the map (8). For $u_1=1$, $u_2=50$, and noise amplitude $\epsilon_0=0.0175$ we find $r_c\approx 1.15$.

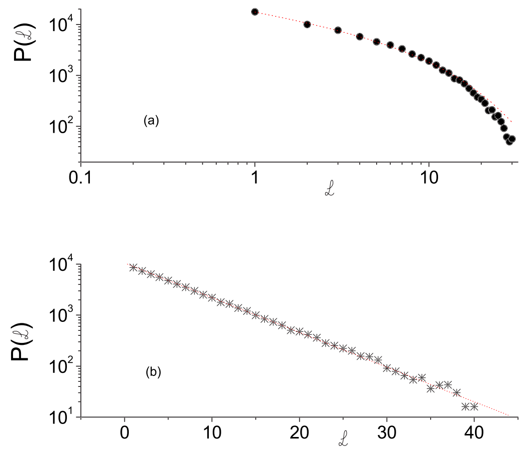

FIG. 6. (Color online) (a) The distribution of the laminar intervals calculated using the map (7) with $r=1.25$, $u_1=1$, $u_2=50$, and $\epsilon_0=0.0175$. (b) The distribution of the laminar intervals calculated using the map (7) with $r=1.4$, $u_1=1$, $u_2=50$, and $\epsilon_0=0.0175$.

Per construction the lower end of the laminar region is $\phi_L=0$. For the upper end we have used $\phi_R=0.14$, however, our results are similar for a wide range of ϕ_R values provided that $\phi_R<0.5$. Fitting using the function (3) leads to $p_2=0.58\pm0.02$ and $p_3=0.1\pm0.006$ in accordance with the above discussion. Increasing r the exponent p_2 decreases while p_3 increases. Thus the distribution $P(\mathcal{L})$ tends rapidly to an exponential form. This is clearly illustrated in Fig. 6(b) where we plot $P(\mathcal{L})$ for the map (8) calculated using $r=1.4$. All the remaining parameters in (8)) have the same values as in Fig. 6(a). It is obvious that the corresponding dynamics are weakly correlated (or even random) in time.

In order to show that the fluctuation pattern described in Fig. 6(a), determined by the conditions $p_2<1$, $p_3\ll 1$ is associated with tricritical behavior we calculate the space averaged magnetization in the $Z(3)$ spin model where three possible orientations of the spin vector are possible [10].

$$\vec{s} \equiv \left\{(1,0),\left(-\frac{1}{2},\frac{\sqrt{3}}{2}\right),\left(-\frac{1}{2},-\frac{\sqrt{3}}{2}\right)\right\}. \tag{9}$$

The different spin states are planar and form in pairs an angle of $\frac{2\pi}{3}$. The Hamiltonian of the system is given by

$$H = J\sum_{\langle i,j\rangle} \vec{s}_i\vec{s}_j, \tag{10}$$

$\langle i,j\rangle$ denoting first neighbors. At high temperature the statistical weights of all three spin orientations are exactly equal.

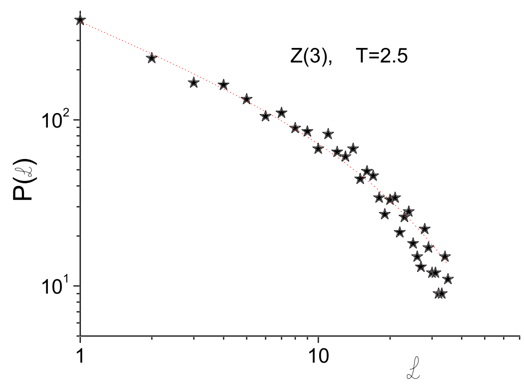

FIG. 7. (Color online) The distribution of the laminar intervals for the $Z(3)$ spin model calculated using a $20\times20\times20$ lattice at $T=2.5$.

As the temperature decreases below a critical value, a narrow zone appears within which the values of the statistical weights fluctuate around 1/3. As the temperature decreases further a preferred spin state emerges while the other two states remain to be equally probable. In the fluctuation region the system posseses the characteristics of a metastable phase combining properties of a first and a second order transition, namely, a tricritical behavior [7]. Using the Metropolis algorithm we have calculated the mean magnetization as a function of time in the fluctuation region of the $Z(3)$ model. In addition we have determined the distribution $P(\mathcal{L})$ of the sizes of the time intervals spent in the linear neighborhood of the magnetization fixed point $\vec{\phi}^*=\vec{0}$. The result of the calculation is shown in Fig. 7. A Monte Carlo trajectory consisting of 220 000 time steps (algorithmic time) on a $20\times20\times20$ lattice at $T=2.5$, below the critical $T_c=2.75$, is used. The fit with the function (4) leads to $p_2=0.59\pm0.03$ and $p_3=0.04\pm0.006$ in close analogy with those obtained through the map (8) [see Fig. 6(a)].

V. CONCLUSIONS

We have developed an approximative scheme in order to describe the order parameter fluctuations in the neighborhood of a critical or a tricritical point. Our approach is based on a previous observation [4] that the order parameter fluctuations of a thermal system at the critical point possess a deterministic component described by an intermittent map. Here we extend the validity of this map in the entire phase diagram region surrounding the critical point. This is achieved by introducing a control parameter in the critical map, which is found to be in one-to-one correspondence with the reduced temperature in a thermal system. We also show that in the case of a tricritical point a consistent description of the fluctuations requires the addition of a nonlinear term in the corresponding effective map. Using the effective dynamics in the broken symmetry phase we predict the existence of a distribution with universal characteristics for the time intervals, spent in the linear neighborhood of the destabilized fixed point. According to this treatment the following picture for the collective dynamics in the critical region is revealed: Exactly at the critical point the system passes through ordered phases characterized by a nonvanishing space averaged magnetization. During such a phase the magnetization, starting from very small absolute values, increases with time as more and more spins align each other. The fluctuations during this laminar phase are small and constitute a noise effect on the dominating increasing behavior. Whenever the absolute value of the total magnetization exceeds some threshold the corresponding configuration becomes extremely unstable and the system makes a sudden transition to a new configuration with much smaller total magnetization absolute value. During the transition phase the fluctuations are large, practically of any size restricted only by the size of the system. Thus, after the transition the total magnetization sign can change. This dynamics leads to a sequence of ordered phases with alternating total magnetization so that the corresponding time average is zero. The time intervals for which each ordered phase (characterized by the regular magnetization increase) survives, are power-law distributed and the associated exponent is determined by the isothermal critical exponent δ. As the state of the system departs slightly from the critical one, a similar scenario holds. The main difference is the appearance of an exponentially decaying factor in the distribution of the laminar lengths, reflecting the breaking of scale invariance in the effective action of the system. Thus, near to the critical point the laminar length distribution is a product of a power-law and an exponential term. The same form applies also for a system near a tricritical point. However, the first order characteristics present in this case lead to a reduction of the fluctuations expressed through a decrease of the exponent in the power-law factor. Although the described statistical properties of the laminar length distribution are extracted through the fictitious dynamics of the Monte Carlo simulation of the 3D Ising and $Z(3)$ model they provide a reasonable scenario for the statistical characteristics of the system evolution in the critical region. Furthermore, the underlying intermittent dynamics derived from these statistical properties, are compatible with the changes in the stability properties of the ground state (due to spontaneous symmetry breaking) during the phase transition.

ACKNOWLEDGMENTS

The present work is co-funded by the European Social Fund and National Resources (EPEAEK II) Pythagoras (Grant No. 70/3/7972).

APPENDIX

Following the standard approach [11] it is straightforward to estimate the distribution of the sizes of the deformed laminar intervals for the map $x_{n+1}=rx_n+ux_n^z$. In the limit $r\to1$ one obtains approximately the following differential equation:

$$\frac{dx}{d\mathcal{L}}=(r-1)x+ux^z. \quad \text{(A1)}$$

Integrating Eq. (A1) we find

$$\int_0^l d\mathcal{L} = \int_{x_0}^{c} \frac{dx}{(r-1)x + ux^z} = \int_{x_0}^{c} \frac{dx}{x[(r-1) + ux^{z-1}]},$$

which after the transformation $x \rightarrow y^{1/z-1}$ becomes

$$\mathcal{L} = \frac{1}{z-1} \int_{x_0^{z-1}}^{c'} \frac{dy}{y[(r-1) + uy]}$$
$$= \frac{1}{(z-1)(r-1)} \left[\int_{x_0^{z-1}}^{c'} \frac{dy}{y} - u \int_{x_0^{z-1}}^{c'} \frac{dy}{(r-1) + uy} \right]$$
$$= \frac{1}{(z-1)(r-1)} \ln\left[\frac{(r-1) + ux_0^{z-1}}{x_0^{z-1}} \frac{c'}{c_2} \right]$$

leading finally to

$$\mathcal{L} = \frac{1}{(z-1)(r-1)} \left[\ln\frac{(r-1) + ux_0^{z-1}}{x_0^{z-1}} + k \right], \quad k = \ln\frac{c'}{c_2}, \tag{A2}$$

where the parameter c' is determined by the initial change of variables and the parameter c_2 is obtained after the last integration.

The distribution of laminar lengths is given as [11]

$$P(\mathcal{L}) \sim \left| \frac{dx_0}{d\mathcal{L}} \right|. \tag{A3}$$

The derivative $|\frac{dx_0}{d\mathcal{L}}|$ can be found using Eq. (A2).

$$\frac{(r-1) + ux_0^{z-1}}{x_0^{z-1}} = e^{\mathcal{L}(z-1)(r-1)-k},$$

$$\frac{r-1}{x_0^{z-1}} = e^{\mathcal{L}(z-1)(r-1)-k} - u,$$

$$x_0 = \left(\frac{r-1}{e^{\mathcal{L}(z-1)(r-1)-k} - u} \right)^{1/(z-1)},$$

leading to the result

$$\left| \frac{dx_0}{d\mathcal{L}} \right| = A \frac{e^{\mathcal{L}(z-1)(r-1)}}{(e^{\mathcal{L}(z-1)(r-1)} - u')^{z/(z-1)}}, \tag{A4}$$

where the parameter A is independent from $\mathcal{L}$ and $u' = ue^k$. Without loss of generality we can put $u' \equiv 1$ getting finally

$$P(\mathcal{L}) \sim \frac{e^{\mathcal{L}(z-1)(r-1)}}{(e^{\mathcal{L}(z-1)(r-1)} - 1)^{z/(z-1)}}. \tag{A5}$$

[1] N. Metropolis, A. W. Rosenbluth, M. N. Rosenbluth, A. H. Teller, and E. Teller, J. Chem. Phys. **21**, 1087 (1953).

[2] K. Binder, *Applications of the Monte Carlo Method in Statistical Physics* (Springer, Berlin, 1984).

[3] M. E. J. Newman and G. T. Barkema, *Monte Carlo Methods in Statistical Physics* (Oxford University Press, New York, 1999).

[4] Y. F. Contoyiannis and F. K. Diakonos, Phys. Lett. A **268**, 286 (2000).

[5] Y. F. Contoyiannis, F. K. Diakonos, and A. Malakis, Phys. Rev. Lett. **89**, 035701 (2002).

[6] Y. F. Contoyiannis, F. K. Diakonos, C. Papaefthimiou, and G. Theophilidis, Phys. Rev. Lett. **93**, 098101 (2004).

[7] K. Huang, *Statistical Mechanics*, 2nd ed. (Wiley, New York, 1987).

[8] Y. F. Contoyiannis, P. G. Kapiris, and K. A. Eftaxias, Phys. Rev. E **71**, 066123 (2005).

[9] Y. F. Contoyiannis, F. K. Diakonos, P. G. Kapiris, A. S. Peratzakis, and K. A. Eftaxias, Phys. Chem. Earth **29**, 397 (2004).

[10] L. A. Fernandez, E. Marinari, G. Parisi, S. Roncolini, and A. Tarancón, Phys. Lett. B **217**, 309 (1989); L. A. Fernandez, U. Marini Bettolo Marconi, and A. Tarancón, *ibid.* **217**, 314 (1989).

[11] H. G. Schuster, *Deterministic Chaos: An Introduction*, 2nd ed. (VCH, Weinheim, 1989).

[12] The singular case of order parameter conserving algorithms should be excluded.

[13] Actually one needs an ensemble with an infinite number of trajectories to determine the distribution of the order parameter at a fixed temperature.